Deep electronic states in ion-implanted Si

EVANS-FREEMAN, J. H., EMIROGLU, D., GAD, M. A., MITROMARA, N. and VERNON-PARRY, K. D.

Published version

EVANS-FREEMAN, J. H., EMIROGLU, D., GAD, M. A., MITROMARA, N. and VERNON-PARRY, K. D. (2006). Deep electronic states in ion-implanted Si. Journal of materials science.

Deep Electronic States in Ion-Implanted Si

J H Evans-Freeman, D Emiroglu, M A Gad, N Mitromara and K D Vernon-Parry

Materials and Engineering Research Institute
Sheffield Hallam University
Howard Street, Sheffield, S1 1WB
United Kingdom

Abstract

In this paper we present an overview of the deep states present after ion-implantation by various species into n-type silicon, measured by Deep Level Transient Spectroscopy (DLTS) and high resolution Laplace DLTS (LDLTS). Both point and small extended defects are found, prior to any anneal, which can therefore be the precursors to more detrimental defects such as end of range loops. We show that the ion mass is linked to the concentrations of defects that are observed, and the presence of small interstitial clusters directly after ion implantation is established by comparing their behaviour with that of electrically active stacking faults. Finally, future applications of the LDLTS technique to ion-implanted regions in Si-based devices are outlined.

Introduction

Ion implantation into Si is still the preferred process for the introduction of dopants, as most of the damage caused can be annealed out, and introduction of atomic concentrations beyond the solid solubility limit is possible. However, as device dimensions and doping requirements become more stringent there is increasing concern about residual damage in the implanted region, the effect of remaining interstitials, and junction integrity. Indeed, some state of the art CMOS transistors, which use doped SiGe as the drain and source regions to provide strain in the channel, currently use doping during epitaxial growth for these regions. This reflects the fact that not enough is known about the damage caused in SiGe by high dose ion implants.

Other problems include the unwanted diffusion of implanted boron. During the annealing of B-implanted Si, the boron initially diffuses at least 100 times faster in the implanted region than in bulk silicon. This fast initial diffusion, or Transient Enhanced Diffusion (TED), leads to broader doping profiles than predicted and can limit the size reduction obtainable in submicron Si-based devices. Interstitial defects in silicon introduced by the implantation and annealing, e.g.{311 defects} and end-of-range dislocation loops, are believed to be the reason for TED in silicon, as B is an interstitial-assisted diffuser. Modelling of the formation of {311} defects shows preferential cluster sizes during the ripening of these extended defects [1], and it has been possible to identify these precursor clusters experimentally by electrical characterisation [2-5]. The problem of TED is now receding as the fabrication process either employs very low energies to form the critical areas, which produce very few extra interstitials, or introduces very rapid anneal schedules. A further solution may lie in the introduction of another ion which promotes vacancy formation or retention, thus reducing the interstitial population, and hence reducing all diffusion. A possible candidate species currently under investigation is F [6], but other elements such as C may also have the same effect.

Point defects created during implantation may subsequently cluster into extended defects, specifically, interstitials may develop into end-of-range dislocation loops. Defects present after implantation, but before annealing, were initially thought to have the same properties as those introduced by electron or proton irradiation of silicon [7-

9], but this has more recently been shown not to be the case [10]. There are significant differences in the effect of the two types of bombardment: ions cause larger collision cascades than protons or electrons, and there is a non-uniform defect distribution when ions are implanted.

It is known that extended defects in silicon often exhibit electrical activity, and that if they do, their behaviour is significantly different from point defects with respect to the carrier trapping and emission process. As carrier capture proceeds into such defects, the capture rate is non-exponential and reduces as the extended defect becomes charged. Capture of carriers also alters the local band structure around the defect, which has been established by Electron Beam Induced Current (EBIC) measurements [11] and Deep Level Transient Spectroscopy (DLTS) measurements [12]. However, DLTS generally yields quite broad peaks from Si containing dislocations, and only limited investigations of activation energies and decoration effects have hitherto been possible.

High resolution Laplace DLTS (LDLTS) [13] overcomes some of these problems, providing information on closely spaced electronic levels in the bandgap by recording and analysing capacitance transients which consist of one or more exponentials. In this paper we review the use of LDLTS to characterise point defects and small clusters in ion-implanted n-type Si, before any annealing, and compared the results with the electrical behaviour of partial dislocations surrounding stacking faults in oxidised Si.

Experimental Techniques

The electrical measurements were carried out on samples implanted with a range of ion doses. Some very low doses were included, of approximately $10^{10}cm^{-2}$, because high doses caused too much carrier removal, due to deep traps, for electrical techniques such as DLTS and capacitance-voltage (C-V) to be carried out before annealing, i.e. on the as-implanted samples. A variety of implant species was used to ascertain the effect of increasing ion mass on the nature of as-implanted defects. The

starting material was n-type CZ silicon with a low resistivity (about 1-2 Ω-cm). An as-supplied wafer was used for reference purposes, and three wafers were implanted at room temperature with silicon (Si:Si), ytterbium (Si:Yb) or erbium (Si:Er). All implants were carried out after the predicted ion ranges had been calculated using the freely available modelling tool Transport of Ions in Matter (TRIM) [14]. The implanted regions were encompassed within the depletion regions occurring at low reverse biases, in order that we could profile through the implanted region electrically. The low doses ensured that there was a minimum of carrier removal due to deep defect states after the implantation. A comparison study of n-type Si, resistivity 2Ω-cm, which was irradiated with protons at 24GeV/c, was carried out. At this irradiation energy, the protons passed right through the sample, as confirmed by TRIM, leaving only residual damage. After implantation or irradiation, aluminium Ohmic contacts were evaporated on the rear face, and gold Schottky contacts were evaporated on the front face. Table I summarises all the sample details, implanted ions and implantation conditions.

Dislocations were also generated in Si by oxygenation to act as a control for the cluster studies, by oxidising Si at 1100°C for one hour. The result of this process was the formation of oxidation-induced stacking faults (OISFs) which consist of extra (111) half planes surrounded by sessile a/3<111> Frank partial dislocations. It has been known for some time that the electrical activity associated with the OISFs actually occurs at the bounding Frank partials [15]. Stacking faults generated for this study had typical mean lengths of a few microns (less than 10) determined by Y3 preferential etch and optical microscopy [16].

DLTS is a quasi-spectroscopic technique widely used by researchers in semiconductors to ascertain the Gibbs free energy of deep electronic energy states within the forbidden energy gap. A diode is placed into zero or forward bias, to ensure that deep electronic levels below the Fermi level are filled (the so-called "fill" pulse), and then placed into reverse bias. During this latter phase, the thermal emission from carriers in traps now above the Fermi level contributes to a transient in the recorded capacitance. This capacitance is sampled at three occasions and analysed with a boxcar integrator. The process is repeated many times as the temperature is gradually swept between, typically, 300K to 70K and back again, and on each temperature sweep the boxcar sampling rate is changed. The result is a series of peaks from which an Arrhenius plot can be created, giving an activation energy. The resolution is quite poor however, with deep level energies typically having error bars of up to 50meV. This poor resolution can be overcome by using the newer technique of Laplace DLTS (LDLTS) [13].

LDLTS records the capacitance transient due to carrier emission at a fixed temperature and applies mathematical algorithms to extract the emission rates present in the transient. A high stability cryostat is therefore required. The choice of temperature is usually dictated by the original DLTS measurement, i.e. a temperature is chosen at which there is a peak in the DLTS spectrum, though other temperatures can be chosen. In principle, any temperature can be used if the experiment is carried out over a long enough period of time to capture small signals due to all emission from all deep centres in the sampled volume but there is an optimum temperature for each deep state, which is around the maximum of the DLTS peak. In LDLTS, if the capacitance transient consists of only one exponential emission rate, due to emission

from a single type of point defect, only one peak is exhibited in the LDLTS spectrum, and the area under each sharp peak is proportional to the concentration of the deep level with that emission rate.

In this work several thousand capacitance transients were averaged, which ensured that the signal-to-noise ratio was ≥ 1000:1, which was necessary to separate transients with closely spaced emission rates. The transient was analysed by the routines in the LDLTS software, and a plot of peak intensity as a function of emission rate produced.

The majority capture cross section σ_n is given by [17]

$$\ln\left[\frac{\Delta C_\infty - \Delta C_t}{\Delta C_\infty}\right] = \sigma_n V_{th} n t_p \qquad (1)$$

where t_p is the pulse length, n is the majority carrier population; V_{th} is the thermal velocity, ΔC_∞ is the equilibrium capacitance value and ΔC_t is the capacitance at time t. In the DLTS technique the pulse length is normally approximately 2-5ms, chosen so that the deep levels are totally filled. However, trap filling can be influenced by the pulse length t: if shortened, eventually incomplete trap filling occurs. According to Equation 1, the majority capture cross-section obeys a linear dependence on the logarithm of a combination of capacitance terms. Deviation from this relationship provides a sensitive test for the presence of extended defects that exhibit the Coulombic repulsion described above, because the repulsive force reduces subsequent carrier capture at the defect. The capture rate therefore becomes dependent upon the amount of charge already captured at the defect(s).

Results and Discussion

When ions are implanted into a semiconductor host, there is compelling evidence that the region between the peak and the surface is richest in vacancies, and the region after the peak towards the end of range is richest in interstitials [18]. The interstitials

have the potential to cluster and form end-of-range or other extended defects during annealing, but it is not known experimentally if small defect clusters are formed prior to an anneal, and whether they exhibit electrical activity. Figure 1 shows the DLTS spectra of Si implanted with protons, Si and Er. The spectrum from the Si implanted with Ge was virtually identical to the Er-implanted one, and is not shown for clarity. It is clear that the ratio of the peak height at approximately 235K to the peak height at 100K is changing. The lighter particles produce a ratio between the two peak heights below 5, whereas the heavier, rare earth ions produce a value two orders of magnitude greater than this. Inspection shows that this peak also changes to a lower temperature by about 10K in the case of the rare earth implant. Because of these differences, we deduce that the overall effect of an ion implant is primarily apparent in the feature at around 235K.

Because of the existence of the vacancy-rich and interstitial-rich regions in implanted silicon, it is important to establish whether the two regions have different electrical signatures in DLTS or LDLTS before continuing to investigate the end of range region. Comparison of Capacitance-Voltage (C-V) data with simulations of the implant profile by TRIM determined that a reverse bias of –2 V and fill pulse of –1 V would examine the vacancy-rich region, and a reverse bias of –5 V and fill pulse of –4 V would examine the interstitial-rich region of the implanted samples. The DLTS profiles look identical, but, as has been explained previously, broad DLTS peaks may often contain much extra detail about closely spaced deep levels. Figure 2 shows the LDLTS of the low dose Er-implanted Si, before annealing. The measurement temperature was 225K. The LDLTS spectra of the vacancy-rich and interstitial-rich regions differ from each other, and neither exhibit of the two lines that would be seen

in proton-irradiated silicon. If protons are implanted, one sees either one or two lines in the LDLTS spectrum at 225K depending upon the doping, due to the singly charged divacancy, VV, and the dopant-vacancy pair, (VP in this case), if the background doping is high enough [7]. Figure 2 shows more than two components in the capacitance transient in both cases: three from the interstitial-rich region and five from the vacancy-rich region. All ion implanted samples in this study showed the same trend of five emission rates in the vacancy-rich region, simplifying to three in the interstitial-rich region. Repeated experiments over several days showed that the results were reproducible, and all emission rates increased with temperature, as should be the case for emission from deep states. However, because the capacitance transient displayed so many components, the trap concentration of each individual deep level was small. Therefore, the signal to noise ratio was quite low, and Arrhenius plots to obtain the activation energies were not possible. The proton-irradiated silicon sample did not exhibit a complex structure in the LDLTS spectra recorded at this temperature. We therefore deduce that this is the peak in the DLTS spectrum which contains the most information about defects in ion implanted Si, and, furthermore, it contains emission from traps present in the vacancy- and interstitial-rich regions.

In order to determine if the interstitial-rich region contains defects that are larger than isolated point defects, the DLTS peak at 225K was measured by DLTS at a reverse voltage of -5V and a fill voltage of -4V, to exclude the vacancy-rich region. The fill pulse duration was varied and the data plotted in accordance with equation 1. Figure 3 shows the results of this exercise for the Er-implanted Si, and it can be seen that the data do not lie on a straight line. However, the data for the proton-irradiated Si lie on a straight line. This sensitive test shows that the defects in this region in the Si:Er

sample are dominated by larger defects which exhibit a time-dependent capture cross-section: i.e. they charge up as they fill with carriers and become progressively more repulsive to further carrier capture.

Figure 4 shows the Arrhenius plots for the stacking faulted sample at three different fill pulse lengths, for a large DLTS peak centred at 250K (not shown). A fill pulse of 0.1ms yields an activation energy of E_c – 420meV, a fill pulse of 1ms yields an activation energy of E_c – 395meV and a fill pulse of 5ms yields an activation energy of E_c – 350meV. Therefore as the fill pulse increases, the apparent depth of the deep level below the conduction band decreases. This can be explained as follows. At the core of the dislocation the conduction band edge is disturbed and rises, increasing the distance between it and the trap level [11]. As deep levels at the dislocation fill, the dislocation core charges up and becomes less attractive to carriers. As time goes by, deep levels that are physically further away from the core fill up, and at these points, in real space, the trap level is nearer to E_C. This modification of the band structure due to dislocations has recently been utilised to obtain light from Si by using local carrier trapping [19]. The stacking faults also exhibit multiple LDLTS lines which change their emission rate with fill pulse length, as shown in Figure 5. The combination of these two results suggests that the dislocations bounding the stacking faults also have a time-dependent capture cross-section, as has been reported previously [12] .

Application to device development

In the future, tighter size tolerances for smaller dimensions in electronic devices will mean that defect control and defect engineering will continue to be major issues in the effort to realise device scaling to produce feature sizes of less than ten of nanometres.

Silicon still dominates the electronics market, itself worth hundreds of billion dollars per year. The dimensions of deep sub-micron silicon-related devices have now shrunk to nano-scale lengths, e.g. a 20nm base width in a SiGe HBT or the <65nm gate length in a MOSFET, i.e. just hundreds of atomic spacings. Such devices require complete understanding and control of effects such as the clustering of impurities or intrinsic defects, defects in novel, compound or strained substrates, vacancy and/or interstitial enhanced diffusion, and the causes of leakage in very highly doped junctions. Si channels in MOSFETS are now often produced with compressive strain by selectively growing doped source/drain (S/D) regions by CVD. These S/D regions are not currently implanted in a commercial process because there is no comprehensive information yet available on the implantation damage introduced into IV-IV compounds. P-well doping is commonly used in transistors before the highly doped, shallow source and drain regions are implanted, but there will be end-of-range damage which extends into the p-well and this is not fully understood. Transient Enhanced Diffusion (and thermal diffusion) of B in Si can be suppressed by F implantation, which may form larger defects that soak up interstitials [6] . However the detailed electrical activity of F clusters (with anything) is yet to be established. These topics can now be tackled by a combination of DLTS and LDLTS, based upon the results from the simpler ion-implanted systems reviewed in this paper.

Conclusions

Samples containing ion implant damage, caused by a variety of ion species, have been characterised by DLTS and high resolution LDLTS. Oxidation induced stacking faults were also generated in identical, un-implanted, silicon to act as a control

sample. In all cases the conventional DLTS showed broad peaks but the LDLTS showed a rich structure of either three or four components in the capacitance transient. Capture cross section measurements on the predominant defect in the end-of-range region in the ion implanted samples show that the end of range defects do not have point-defect-like properties. They have capture behaviour typically associated with larger (more than one atom) defects, and the capacitance change is linearly dependent upon the logarithm of the fill pulse length. It has also been possible, using LDLTS, to observe the same effect in the stacking fault control sample,,i.e. the boundary dislocations of the stacking faults exhibit emission rates which are dependent upon the fill pulse length. The electrical behaviour of the defects in the end-of-range region of ion-implanted samples has therefore been shown to be the same as that of much longer extended defects. This paves the way for studies of problems arising from multiple implants typically carried out in silicon processing for electronic devices at or near the ITRS timeline.

Acknowledgements

We should like to acknowledge Surrey University in the UK for the ion implantations. Part of this work was funded by the United Kingdom Engineering and Physical Sciences Research Council (EPSRC). KVP acknowledges the support of EPSRC through the Advanced Research Fellowship scheme.

References

[1] G. Mannino, N. E. B. Cowern, F. Roozeboom, and J. G. M. van Berkum, Appl. Phys. Lett., 76 (2000) 855.

[2] S. Libertino, S. Coffa S, and J. L. Benton, Phys. Rev. B, 63 (2001) 195206

[3] B.G. Svensson, C. Jagadish, A. Hallen, and J. Lalita, Phys. Rev. B, 55 (1997) 10498

[4] P. Pellegrino, N. Keskitalo, A. Hallen, and B. G. Svensson, Nucl. Instr. Meth. B, 148 (1999) 306

[5] N. Abdelgader and J. H. Evans-Freeman, J. Appl. Phys., 93 (2003) 5118

[6] H A W El Mubarek, J M Bonar, G D Dilliway, P Ashburn, M Karunaratne, A F Willoughby, Y Wang, P L F Hemment, R Price, J Zhang and P Ward, J Appl Phys 96 (2004) 4114

[7] G.D. Watkins and J.W. Corbett, Phys. Rev. 138 (1965) A543

[8] M.T Asom, J.L. Benton, R. Sauer and L.C. Kimerling, Appl. Phys. Lett. 51 (1987) 256

[9] J. Lalita , B.G. Svensson, C. Jagadish and A. Hallen, Nucl. Instr. and Meth. B 127/128 (1997) 69

[10] J.H. Evans-Freeman, P.Y.Y. Kan and N. Abdulgader, J. Appl. Phys. 92 (2002) 3755

[11] P.R. Wilshaw and G.R. Booker, Proceedings of the Microscopical Society Conference, (1985) 329

[12] Y.Qian, J.H.Evans and A.R.Peaker, Inst. Phys. Conf. Ser. No. 134 (1993) 121

[13] L. Dobaczewski, P. Kaczor, I. Hawkins, and A. R. Peaker, J. Appl. Phys.76 (1994) 194

[14] J. F. Ziegler, J. P. Biersack and U. Littmark, "The Stopping and Range of Ions in Solids" Pergamon, New York, 1985; http://www.srim.org/

[15] A. Ourmazd, P. R. Wilshaw and G. R. Booker, Physica B **116**, 600 (1983)

[16] K. H. Yang, J. Electrochem. Soc. **131**, 1140 (1984)

[17] D.V. Lang, J. Appl. Phys. **45**, 3023 (1974)

[18] P. Pellegrino, P. Leveque, J. Wong-Leung, C. Jagadish and B. G. Svensson, Appl. Phys. Lett. **78**, 3442 (2001)

[19] M. A. Lourenco, M. S. A. Siddiqui, G. Shao, R. M. Gwilliam and K. P. Homewood, Phys. Stat. Sol. A 201 (2004) 239

Table 1 Samples used in this work

sample name	implanted ion	Dose (cm^{-2})	implant energy (MeV)	carrier concentration after implantation (cm^{-3})
Si: Si	Si	1×10^{10}	0.8	2.3×10^{15}
Si:Er	Er	1×10^{10}	2	2.7×10^{15}
Si:Ge	Ge	1×10^{10}	2	2.3×10^{15}
Si:p	protons	1×10^{11}	24GeV/c	6.0×10^{15}

Figure Captions

Figure 1 DLTS of Er-and Si-implanted Si, and proton-irradiated Si.

Figure 2 LDLTS of low dose Er-implanted Si, before annealing. The measurement temperature was 225K and the experiments were carried out at two voltage ranges: a reverse bias of –2 V and fill pulse of –1 V which samples the vacancy-rich region, and a reverse bias of –5 V and fill pulse of –4 V which samples the interstitial-rich region.

Figure 3 The capacitance transient height plotted as a function of DLTS fill pulse duration, in accordance with equation 3, for Si:p, irradiated with protons (●) and low dose Er-implanted Si, (+).

Figure 4 Arrhenius plots of Si containing stacking faults at fill pulses 0.1ms (—) with E_a = 420meV, 1ms (- - -) with E_a = 395meV and 5ms (— - -) with E_a = 350meV.

Figure 5 LDLTS of the stacking fault sample at fill pulses of 5ms (—) and 1ms (- - -).

Figure 1

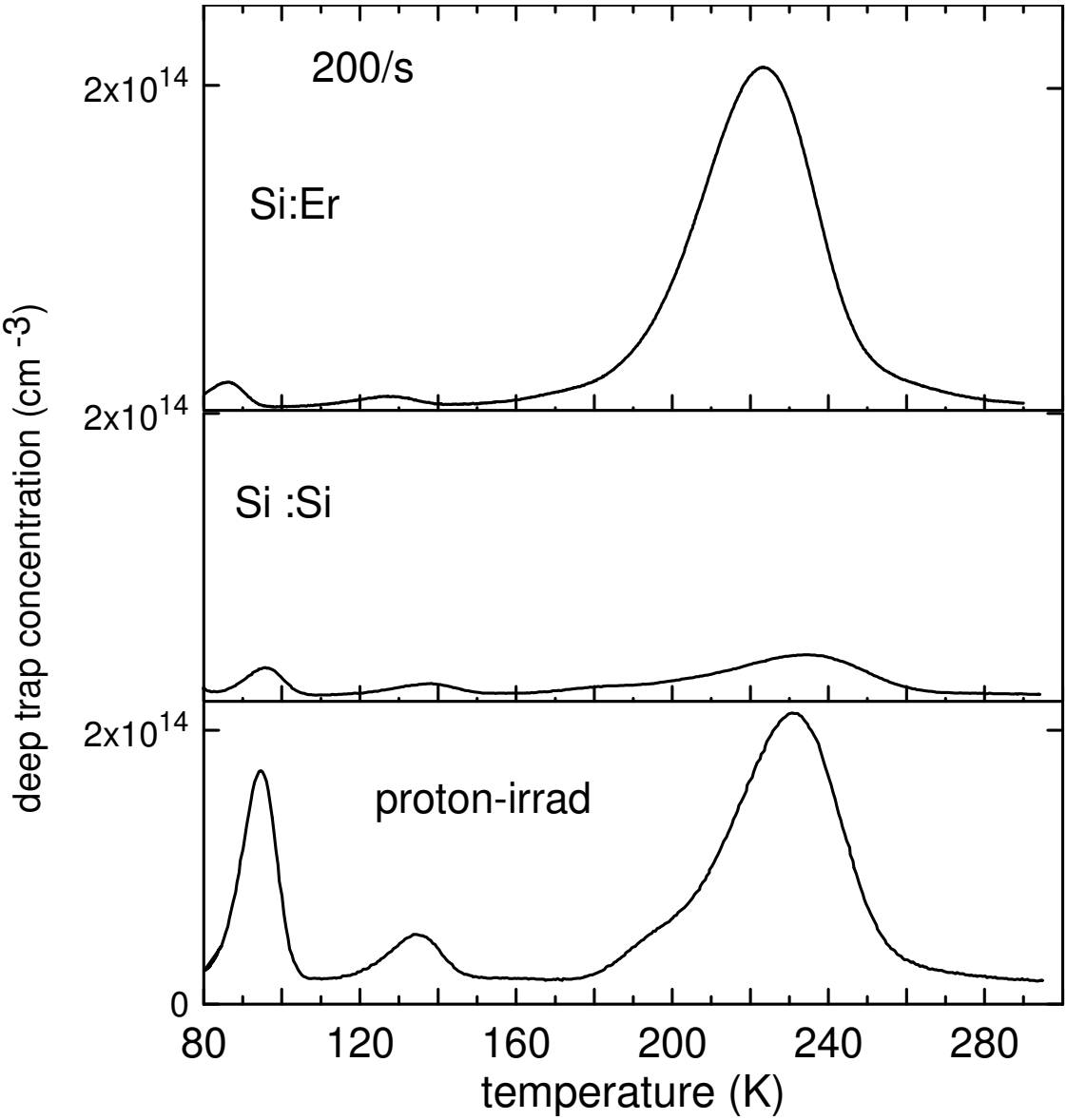
200/s
Si:Er
Si :Si
proton-irrad
2x10^14
2x10^14
2x10^14
0
deep trap concentration (cm -3)
80
120
160
200
240
280
temperature (K)

Figure 2

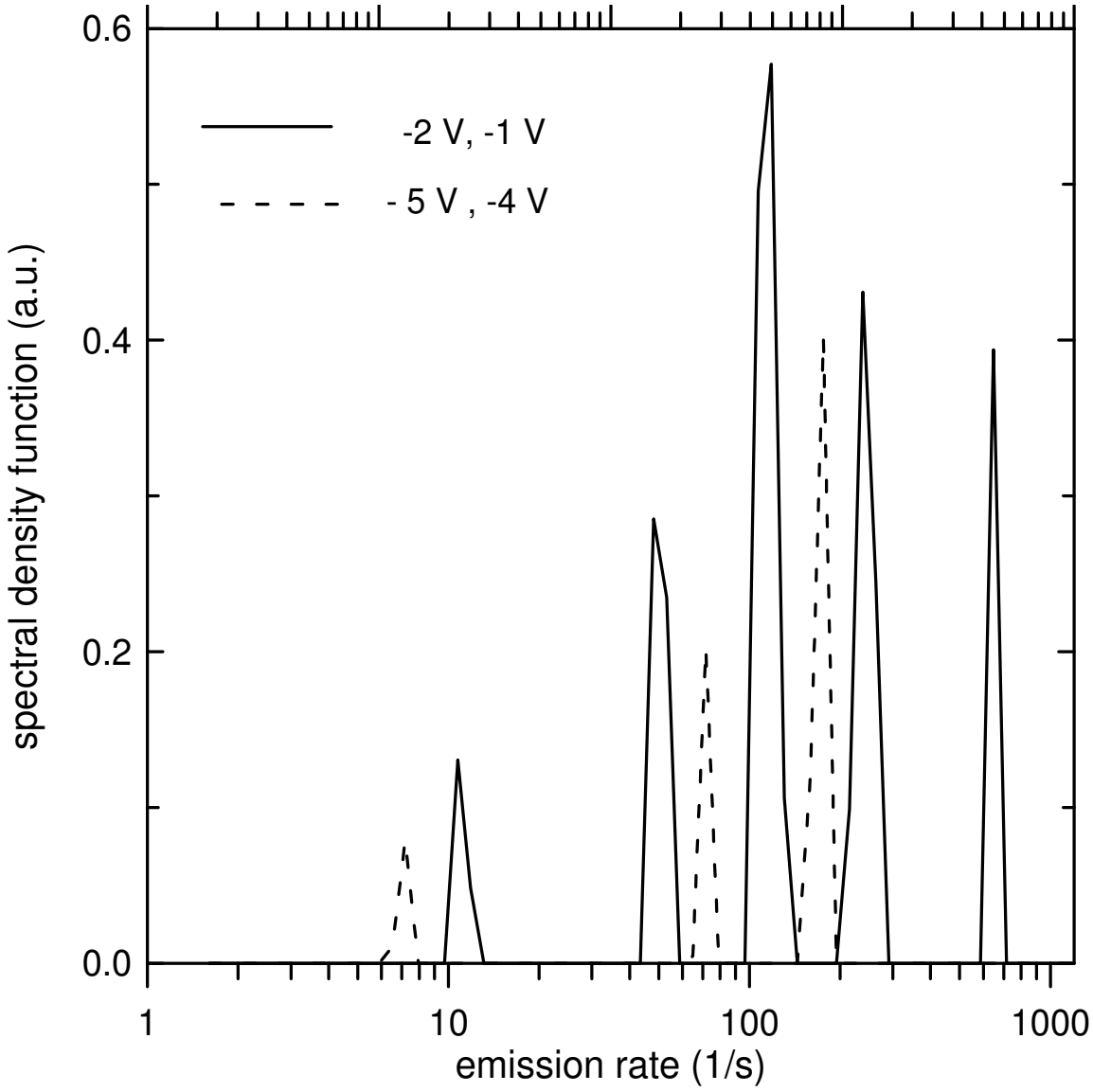
0.6
0.4
0.2
0.0
spectral density function (a.u.)
-2 V, -1 V
- 5 V , -4 V
1
10
100
1000
emission rate (1/s)

Figure 3

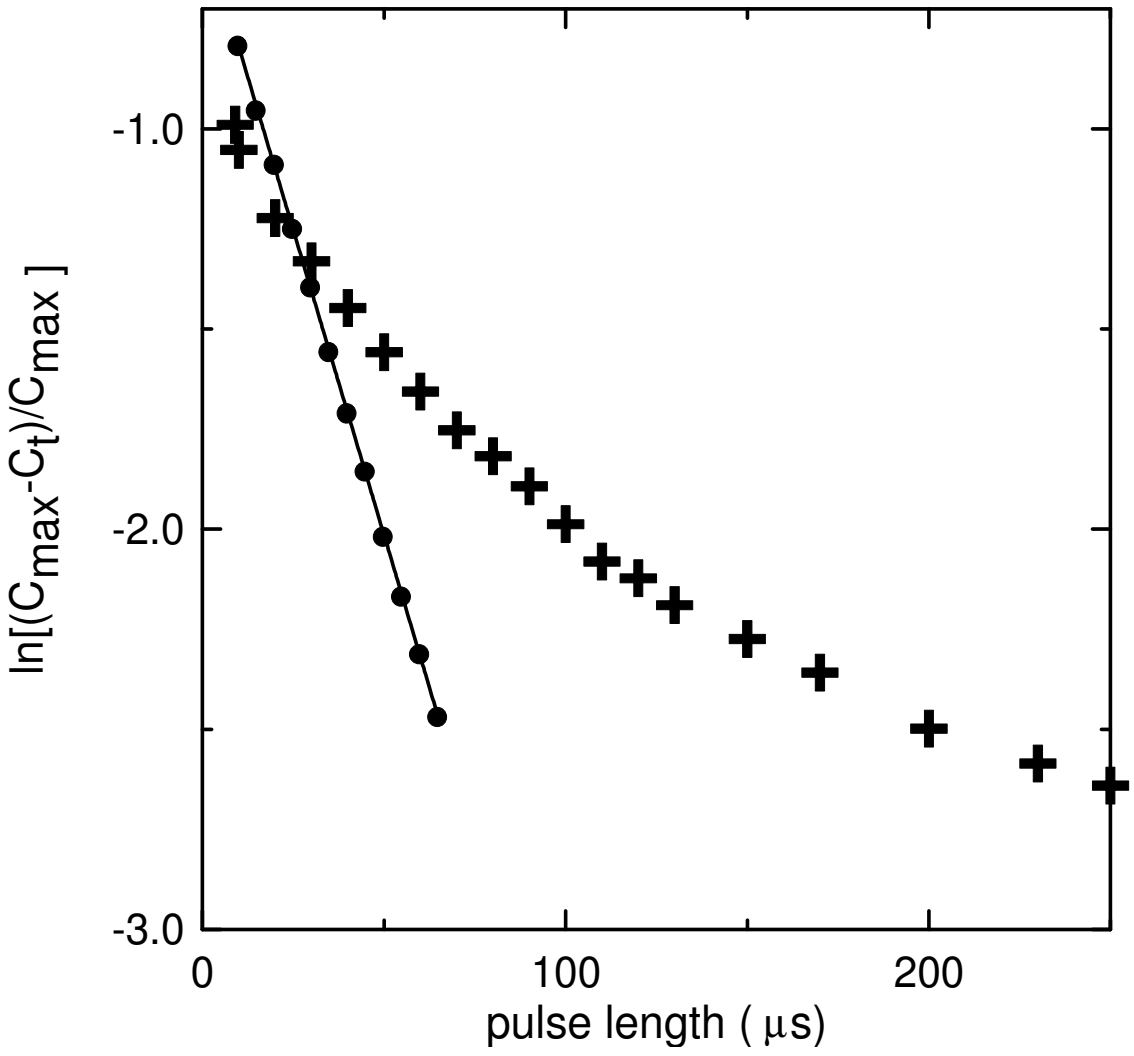

Figure 4

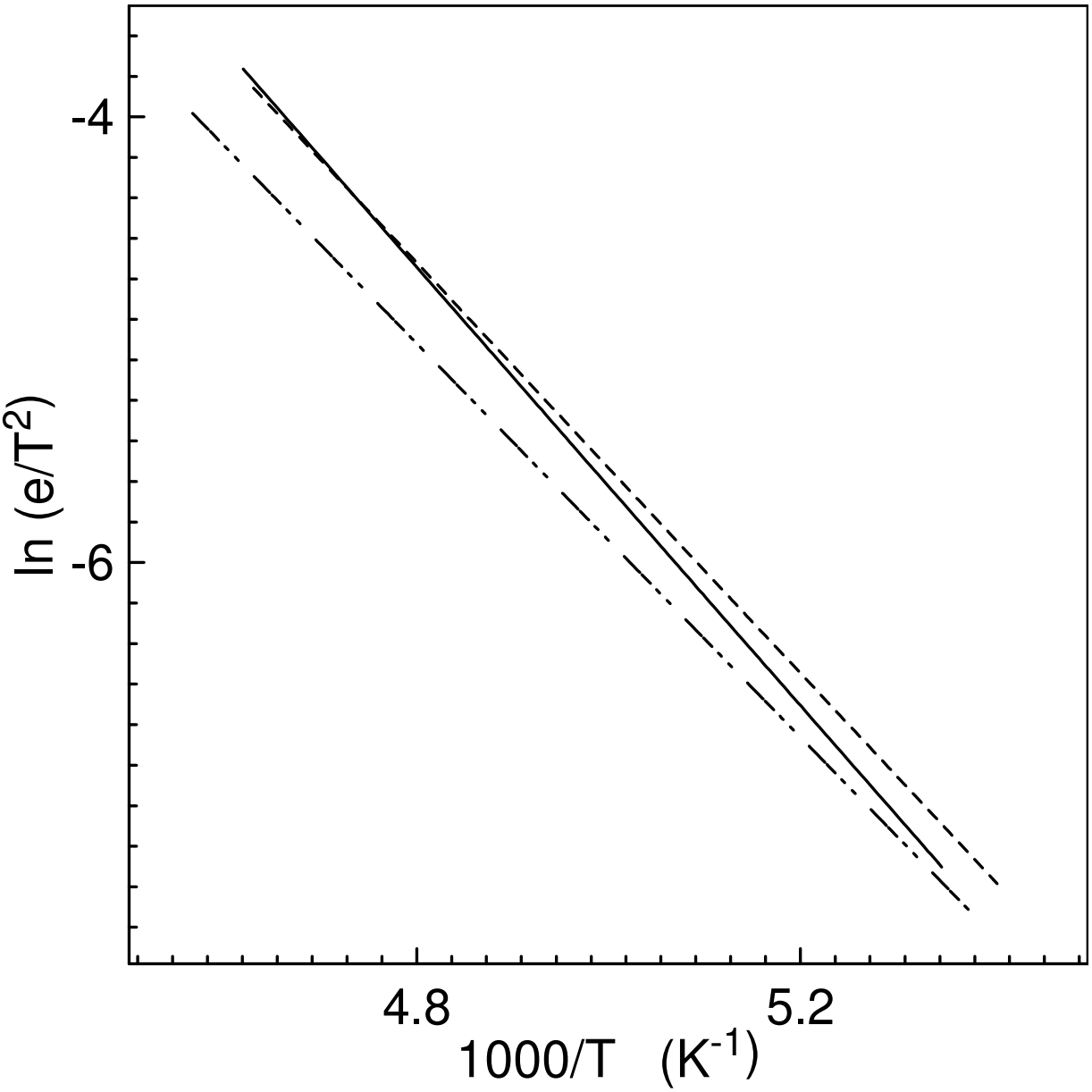

Figure 5

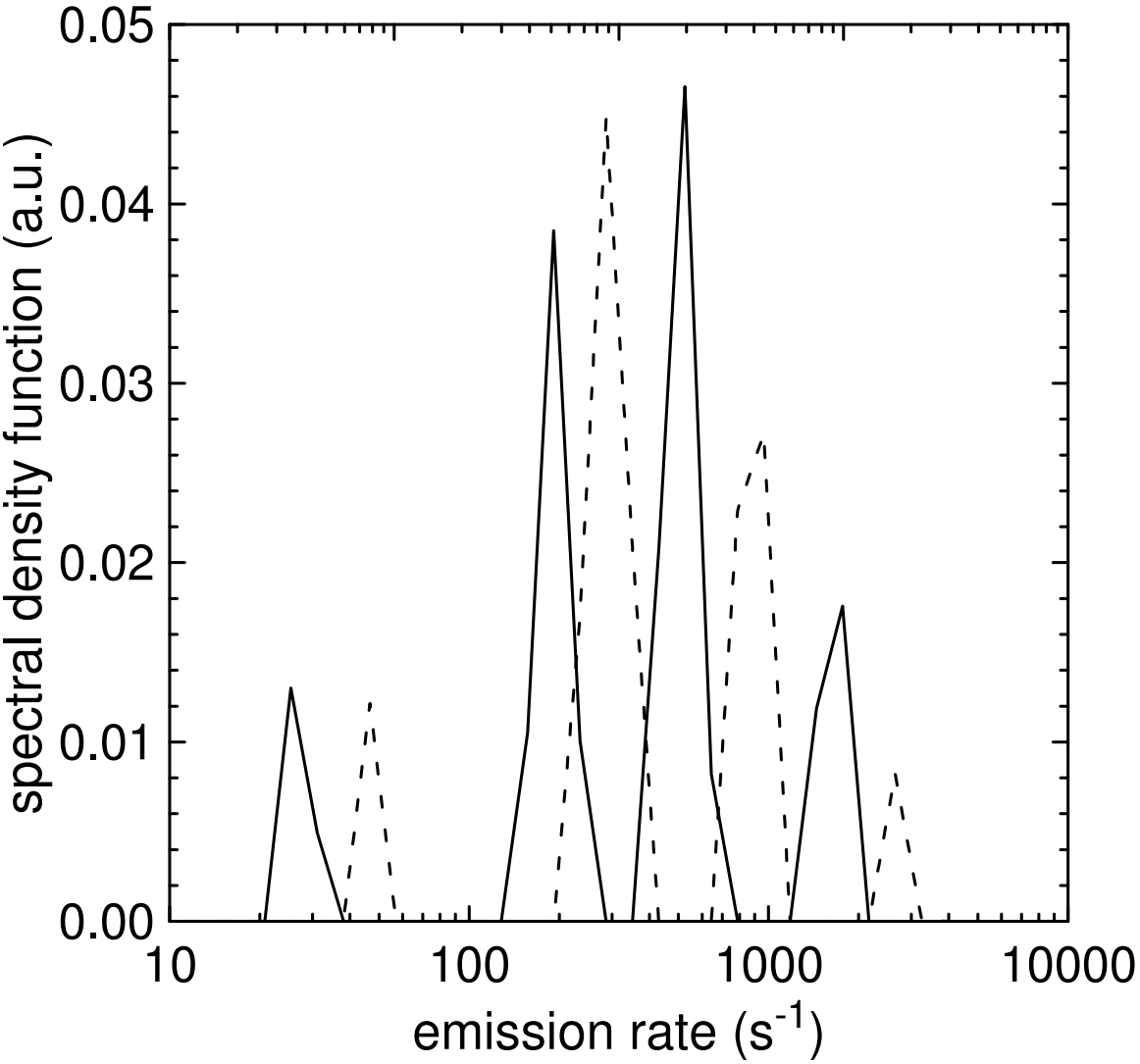
0.05
0.04
0.03
0.02
0.01
0.00
spectral density function (a.u.)
10
100
1000
10000
emission rate (s-1)